Clay Minerals, (2015) **50**, 163–183

Pedogenic, palustrine and groundwater dolomite formation in non-marine bentonites (Bavaria, Germany)

M. H. KÖSTER* AND H. A. GILG

Lehrstuhl für Ingenieurgeologie, Technische Universität München, Arcisstr. 21, 80333 Munich, Germany

(*Received 25 September 2014; revised 20 January 2015; Associate Editor: Helge Stanjek*)

ABSTRACT: Dolomite and calcite in Bavarian bentonites, southern Germany, were investigated using petrography, field-emission scanning electron microscopy and stable isotope geochemistry to explore the role of authigenic carbonate formation during bentonitization. Pedogenic, palustrine and groundwater carbonates were distinguished on the basis of X-ray diffraction, micromorphological and stable isotope analysis. The $\delta^{13}C_{V\text{-}PDB}$ and $\delta^{18}O_{V\text{-}PDB}$ values of dolomite range from −8.0‰ to −6.1‰ and −5.4‰ to −3.4‰, respectively. Calcites show a range from −11.9‰ to −8.1‰ for carbon and from −9.1‰ to −6.2‰ for oxygen. Carbon isotope compositions imply a C3-plant-dominated carbon source and repeated wetting and drying cycles. The oxygen isotope data points to an evaporation and temperature controlled $\delta^{18}O_{V\text{-}SMOW}$ value of meteoric water of −7.0‰ to −4.8‰. A syngenetic to early diagenetic timing of dolomitization is indicated, suggesting both dolomite and bentonite formation in non-saline, non-arid and repeatedly partially-oxygenated and reducing soil and groundwater environments during pedogenesis.

KEYWORDS: bentonite, smectite, dolomite, calcite, palaeosol, freshwater environment.

Bentonite, a versatile and highly priced commodity, is a smectite-rich clay that is commonly formed by alteration of volcanic glass (e.g. Christidis & Huff, 2009). Many world-class bentonite deposits were formed from rhyolitic pyroclastites, although acidic precursor rocks are considered less suitable for bentonitization than intermediate volcanic rocks, such as andesite or latite, due to their high Si to Al ratios and low Mg content (Grim & Güven, 1978; Christidis, 2008). Rhyolitic rocks require intense leaching of silica and alkalis to prevent secondary silica precipitation, as well as the addition of Mg ions to form montmorillonite (Christidis & Dunham, 1997). Thus, many rhyolite-based bentonite deposits are hosted in marine settings. The necessary high water-rock ratios are related either to hydrothermal convection of marine fluids in volcanic complexes for proximal bentonites, e.g. Cabo de Gata, Spain (Delgado, 1993; Delgado & Reyes, 1993), and Milos, Greece (Decher *et al*., 1996; Christidis, 2008), or to compaction-driven diagenetic fluid flow of marine pore waters in sedimentary basins for distal bentonites, e.g. Wyoming, USA (Gilg & Rocholl, 2009). Therefore, seawater is generally considered as the main source for Mg in smectite formed from rhyolitic precursor rocks (Christidis & Huff, 2009). In contrast, bentonite deposits in southern Germany are derived from Mid-Miocene rhyolitic ash deposited in a strictly non-marine freshwater environment. These bentonites often contain abundant dolomite and calcite (Vogt, 1980; Unger, 1999; Ulbig, 1999) with a hitherto unknown temporal and genetic relationship.

Dolomite and calcite in bentonites have been investigated systematically only for the proximal

* E-mail: mathias.koester@tum.de
DOI: 10.1180/claymin.2015.050.2.02

deposits of Cabo de Gata, Spain and Milos, Greece. Both bentonite deposits are related to marine depositional environments in the vicinity of the Mediterranean Sea (Delgado, 1993; Delgado & Reyes, 1993; Decher *et al*., 1996) that could have acted as a source of Ca and Mg. Stable oxygen and carbon isotope studies indicate that in both cases the carbonates did form from hydrothermal mixed marine-meteoric waters at temperatures of ~30 to 90ºC (Delgado, 1993; Delgado & Reyes, 1993; Decher *et al*., 1996).

In contrast, carbonate formation in distal non-marine and non-hydrothermal bentonites is still unexplored, but might shed light on smectitization in such an environment. In this study, we report on the presence of authigenic dolomite and calcite in a non-marine bentonite. Petrographic and isotope geochemical data are used to explore carbonate genesis in this unusual setting and its relationship to bentonitization.

GEOLOGICAL SETTING

The Bavarian bentonite deposits near Landshut, Bavaria (Fig. 1), form the largest bentonite district in Central Europe with a production of 350,000 t/y and a mining history dating back 110 years (Unger, 1999). The bentonite deposits are located in a 40 km × 10 km wide belt (Fig. 1) and are mostly restricted to the Landshut-Neuöttinger Hoch, a tectonic block bordered by NW–SE striking fault zones (Unger, 1999) that were active during the Permian and Cretaceous, and were possibly re-activated during the Tertiary (Lemcke, 1973).

More than 130 individual deposits are hosted in the Mid-Miocene Upper Freshwater Molasse (UFM), the uppermost of four sedimentary sequences that comprise the Cenozoic sedimentary infill of the North Alpine Foreland Basin (NAFB) (e.g. Abdul Aziz *et al*., 2009). The westward dewatering (Lemcke, 1973) clastic sedimentary environment of the NAFB was characterized by meandering rivers, floodplains, high groundwater levels in topographic depressions or oxbow lakes and the formation of gravels, sands and marls (Schmid, 2002). With an estimated overburden of 200 to 300 m, the UFM was not subject to significant burial or high temperatures (e.g. Lemcke, 1973; Ulbig, 1999).

Bentonites in the main bentonite horizon occur as small, irregular lenses of variable size (Vogt, 1980; Ulbig, 1999) hosted by marly floodplain sediments

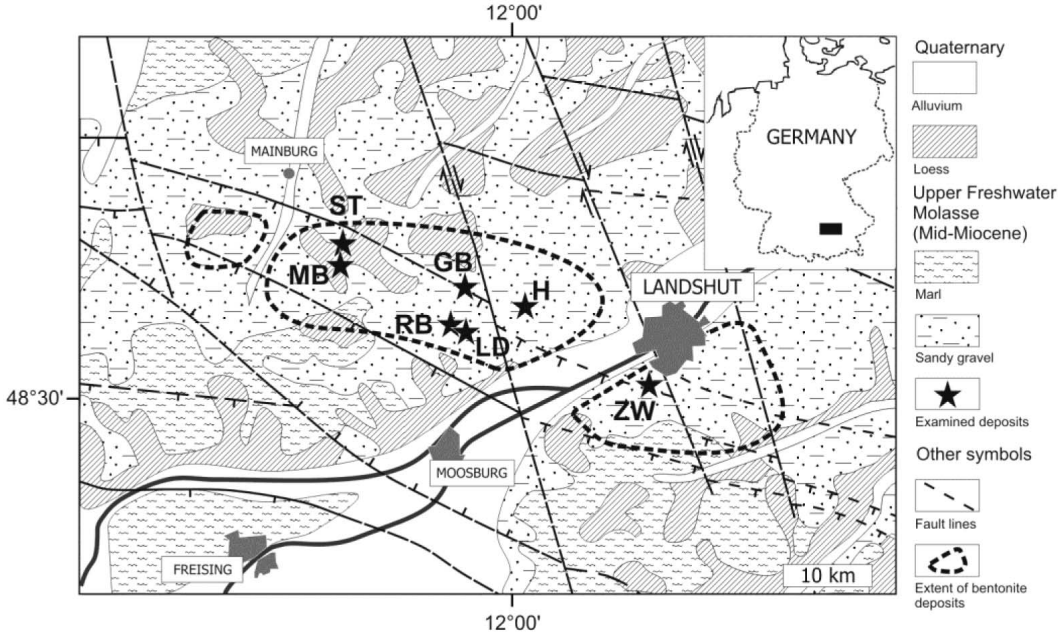

FIG. 1. Simplified geological map (modified from Freudenberger & Schwerd, 1996 and Unger, 1999) and location of the Bavarian bentonite deposits studied.

https://doi.org/10.1180/claymin.2015.050.2.02 Published online by Cambridge University Press

of the Sand–Mergel–Decke (e.g. Abdul-Aziz *et al*., 2009) and/or by fluviatile sand and gravel of the uppermost Nördlicher Vollschotter ~10–30 m above the ejecta layer of the Early Badenian Ries meteorite impact. Hofmann (1973) showed that the bentonites in the Sand–Mergel–Decke share the same lithostratigraphic position as dolomite-bearing "Süßwasserkalke", freshwater limestones and marls with a pronounced and increasing dolomite content at the top and often with a calcareous base. Non-economic bentonites are also found below the ejecta layer of the Ries impact (Ulbig, 1999). Deposits may be discordantly capped by sandy gravel, silt- and mica-rich sand or more rarely by clayey sediment. All fine-grained host-sediments and some gravels show various stages of palaeosol development and are rich in authigenic carbonate (Schmid, 2002).

Ulbig (1999) proposed two types of bentonite deposits formed in different morphological locations to explain sedimentological differences. While the more common deposits of the "Hochlage" (topographic high) are often carbonate-rich clays with marly to clayey footwalls of the Sand-Mergel-Decke, the less common "Tieflage" (topographic low) deposits are usually hosted by sand or gravel and may contain basal kaolinite-rich beds or kaolinite aggregates in bentonite (Ulbig, 1999). The deposits in topographic lows can be completely devoid of carbonates. Intermediate forms of the two types also exist.

The blue, green, grey and yellow bentonites show a bed thickness of 0.5 to 4 m, while total thickness of a deposit may reach 10 m due to often intercalated lithified sub-economic horizons of smectite-poor and partially altered tuffite, sandy clay, or silicified bentonite ("Harte Platte"). The mineralogical composition of bentonites is dominated by Ca-montmorillonite and variable amounts of illite/mica, kaolinite, chlorite, quartz, feldspar, calcite and dolomite, apatite, zircon, Fe-Ti-oxides, occasional glass shards, pyrite and detrital minerals, including epidote and garnet (Vogt, 1980; Ulbig, 1999).

MATERIALS AND SAMPLE ORIGIN

Field work was conducted between 2011 and 2014 in seven actively mined bentonite deposits (Fig. 1). Deposits are located in the Mainburg-Landshut region, Germany, and include the Zweikirchen (ZW), Gabelsberg (GB), Rehbach (RB), Landersdorf (LD), Mittersberg (MB), Hader (H) and Strass (ST) deposits. Eighty two carbonate samples were recovered from bentonites. A carbonaceous wood fragment from the hanging-wall gravels of the reclaimed Peterswahl deposit several kilometers south of Mittersberg was also analysed.

METHODS

Palaeosol development with carbonate accumulations in bentonites are recognized based on horizonation, soil fabrics, root casts and redoxi-morphic features (e.g. Retallack, 1988; Nettleton *et al*., 2000; Schmid, 2002). Carbonate facies are addressed using the schemes of Wright & Tucker (1991), Freytet & Verrecchia (2002) and Alonso-Zarza (2003). Selected samples of each facies were air-dried and hardened in Araldite epoxy resin and cut. The micro-fabrics of the carbonates were examined as standard petrographic thin-sections (~30 μm thick) using a polarizing microscope (Leica DMLM). Air-dried whole-rock samples (not hardened with epoxy resin) were examined with a field-emission scanning electron microscope (FE-SEM) Zeiss Ultra 55 Gemini with a Bruker XFlash 5030 detector and *Quantax Esprit 1.9* software system. The EDX measurements of uncoated samples made it possible to differentiate smectite from dolomite by comparing the relative amount of silica, aluminium, calcium, magnesium and especially carbon. The mineralogical composition was investigated by powder X-ray diffraction analysis from 2 to 70º2θ (Phillips PW 1800, Cu$K\alpha$). The Rietveld program *BGMNwin 1.8.6.* was used for phase quantification. The clay minerals were identified additionally on air-dried, glycolated and heated (550ºC) oriented mounts. Stable isotope measurements were performed with a Con-Flow DeltaPlus (Thermo Scientific) isotopic-ratio mass spectrometer linked to a Gasbench II (Museum of Natural Sciences, Berlin, and GeoBio-Center LMU, Munich, Germany). Isotope ratios are reported as δ-values permil (‰) relative to Vienna Pee Dee Belemnite (V-PDB) with an estimated accuracy and precision of ±0.1‰. 103% phosphoric acid was added drop-wise to each sample with a syringe. Samples were measured after a reaction time of at least 3 h at 72ºC. Standard samples: National Bureau of Standards NBS 18 (carbonatite) and NBS 19 (TS-limestone) and an internal laboratory standard (Solnhofen Plattenkalk: $\delta^{18}O_{V\text{-}PDB}$ of −4.84‰ and $\delta^{13}C_{V\text{-}PDB}$ of −0.47‰), were included in every

https://doi.org/10.1180/claymin.2015.050.2.02 Published online by Cambridge University Press

batch. All three standards show standard deviations of ±0.08‰ for oxygen and ±0.07‰ for carbon. The $\delta^{18}O$ values of dolomite were corrected using a phosphoric acid fractionation factor of 1.00986 at 72ºC (Rosenbaum & Sheppard, 1986).

The calcite-CO_2 and calcite-HCO_3^- carbon isotope fractionation factors of Romanek *et al.* (1992) were used. The carbon isotope fractionation factor of Sheppard & Schwarcz (1970) was applied to estimate the calcite-dolomite fractionation. Deines (2004) showed by theoretical computations that the high-temperature (100−650ºC) dolomite-calcite carbon calibration of Sheppard & Schwarcz (1970) can be extrapolated to low temperatures.

The dolomite-water $^{18}O/^{16}O$ fractionation factor (equation 1) for microbial dolomite (Vasconcelos *et al.*, 2005) and the calcite-water fractionation factor (equation 2) of Kim & O'Neil (1997) were used to determine the oxygen isotopic composition of water:

$$1000 \ln\alpha_{\text{dolomite-water}} = 2.73 \times 10^6 T^{-2} + 0.26 \quad (1)$$

$$1000 \ln\alpha_{\text{calcite-water}} = 18.03 \times 10^3 T^{-1} - 32.42 \quad (2)$$

with T in Kelvin.

RESULTS

Field relationship

Examined bentonite deposits rest on marl, silt or clayey sand of the Sand-Mergel-Decke and show a sharp footwall contact. One deposit (H) underlain by gravels is most likely located in the uppermost Nördlicher Vollschotter gravel. All deposits show a sharp hanging-wall contact and are capped discordantly by younger sediments. Carbonates in bentonites are present as soft and indurated masses, stringers or networks, coalescent nodules, concretions, rhizoliths and cements (Fig. 2). Carbonate content increases towards the hanging-wall and root traces are well preserved, especially in partially altered tuffite (Fig. 5a) and all bentonites show a distinct horizonation and various states of oxidation. Two typical end-members representative of the wide spectrum of carbonate-bearing bentonites are depicted in Figs 2 and 4.

Deposits with pedogenic carbonate

In pedogenic-dominated bentonite deposits, dolomite is abundant in strongly mottled bentonite beds especially in the upper part of the deposit (at Zweikirchen (ZW) (Fig. 2) and also the LD, ST and H (Fig. 1)) where rootlet-associated laminar carbonate networks and carbonate in slickensides are also most frequent. Clastic-filled or dolomite-rich rhizoliths are common in bentonite beds with dolomite nodules. They show well-preserved downward branching root-casts (Fig. 5a) and/or ferruginized rootlets. Shrinkage and desiccation cracks are typical features of dolomite nodules (Fig. 3a) and are also found in the microfabrics as circumgranular cracks and brecciation features (Fig. 3c). Well-preserved root fabrics (Fig. 3b), coalescent nodules, occasional peloids, abundant calcite spar-filled cracks (Fig. 3c), aureoled grains and iron/manganese oxide stains (Fig. 3a) are characteristic and found in various intensities and amounts in all pedogenic dolomites.

Dolomite occurs mostly as subhedral and subrhombic grains of 0.5−5 μm or as round, crypto-crystalline, un-coated, non-broken peloids with a diameter of 80−100 μm as defined by Alonso-Zarza (2003). In samples from the ZW deposit, sub-micron sized elongated "rice" grains and aggregates are observed (Fig. 3d). They are strikingly similar to dolomite precipitated by moderately halophilic aerobic bacteria (Sánchez-Román *et al.*, 2011) or to sub-rounded dolomite aggregates in sub-oxic to oxic Pliocene lacustrine dolomite of the La Roda "white earths" in Spain (García del Cura *et al.*, 2001).

Deposits with palustrine carbonate

In palustrine settings, dolomite (Fig. 4) is located in the upper part of bentonites as irregular masses (RB, MB) or as up to 1.0 m thick nodular horizons (GB) with only incipient mottling. These nodular dolomite beds are found exclusively in palustrine settings and consist of hard and soft, slightly mottled carbonate with small rootlet-traces, clay cutans, and grey, carbonate-free clayey patches. Some bentonite deposits with palustrine carbonate (GB) are host to several meters of partially altered tuffite with abundant root casts (Fig. 5a). Dolomite-lined root-casts are rarely present in partially altered tuffite (MB). In these deposits (GB, MB) rust-red to yellow joint surfaces penetrate downward into bentonite.

The microfabrics are similar to pedogenic dolomite, but show more intense soil churning and pedoturbation (Fig. 5b) through rare shrinkage cracks, crystal-sized mottling, broken bioclasts and tiny, now clay-filled, rootlets.

https://doi.org/10.1180/claymin.2015.050.2.02 Published online by Cambridge University Press

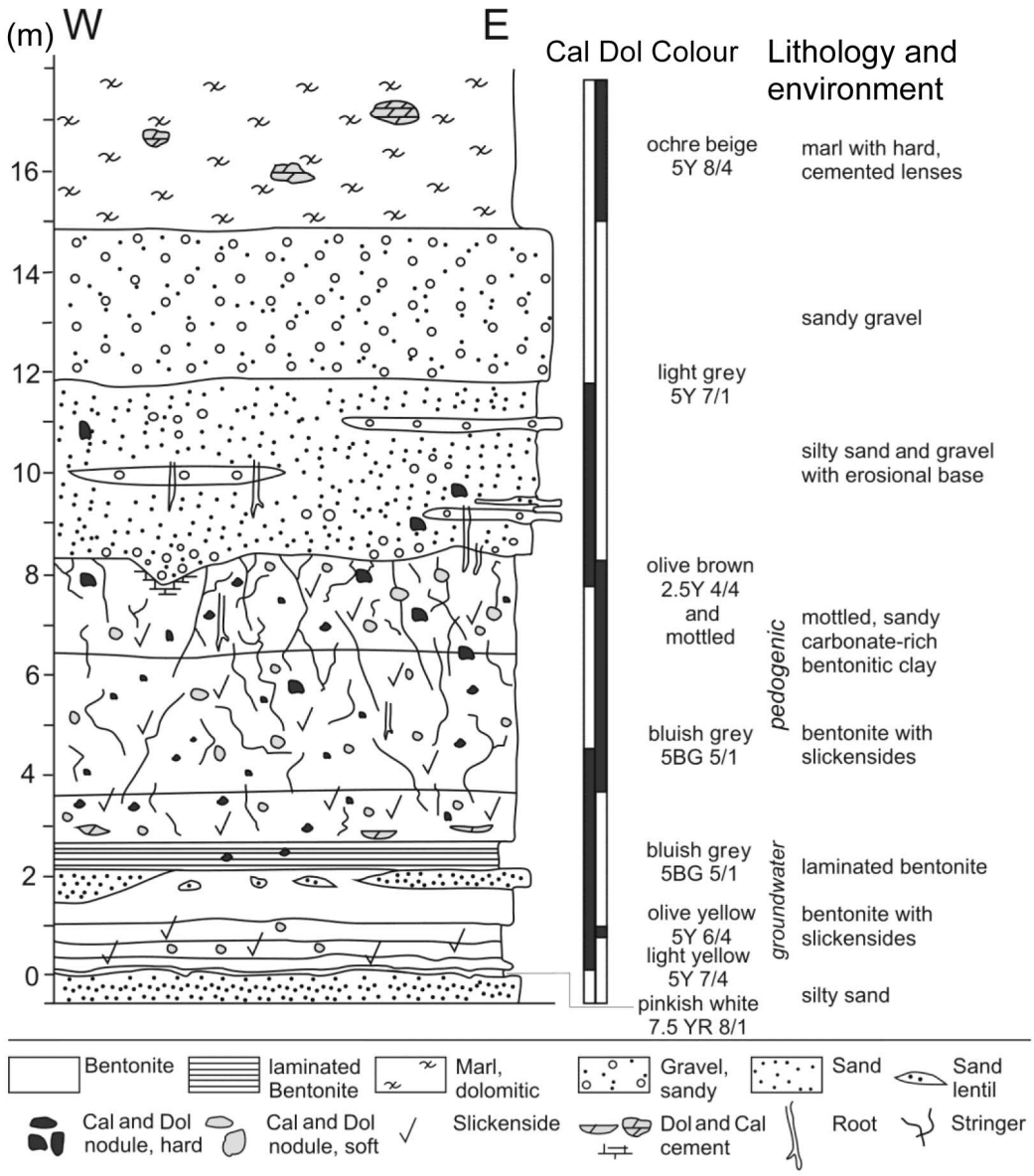

FIG. 2. Section of a pedogenic carbonate-dominated bentonite (Zweikirchen deposit). Cal = calcite, Dol = dolomite.

The micromorphology is also similar to that of the pedogenic facies. An intimate intergrowth of smectite and granular dolomite with a grain size of 50 to 500 nm (Fig. 5c) is commonly observed. Primary volcanogenic, detrital and biogenic particles are replaced by granular dolomite and smectite. Smectite coats detrital grains and glass shards with a dense "sod" of flakes and aggregates, probably indicating direct precipitation from solution. The partially altered tuffite contains abundant glass shards, smectite, rare silified plant remains and small spheres of an undetermined silica phase (Fig. 5d), that indicate the mobilization of silica. Smectite can be found originating from within and more commonly growing on the surface of silica globules.

https://doi.org/10.1180/claymin.2015.050.2.02 Published online by Cambridge University Press

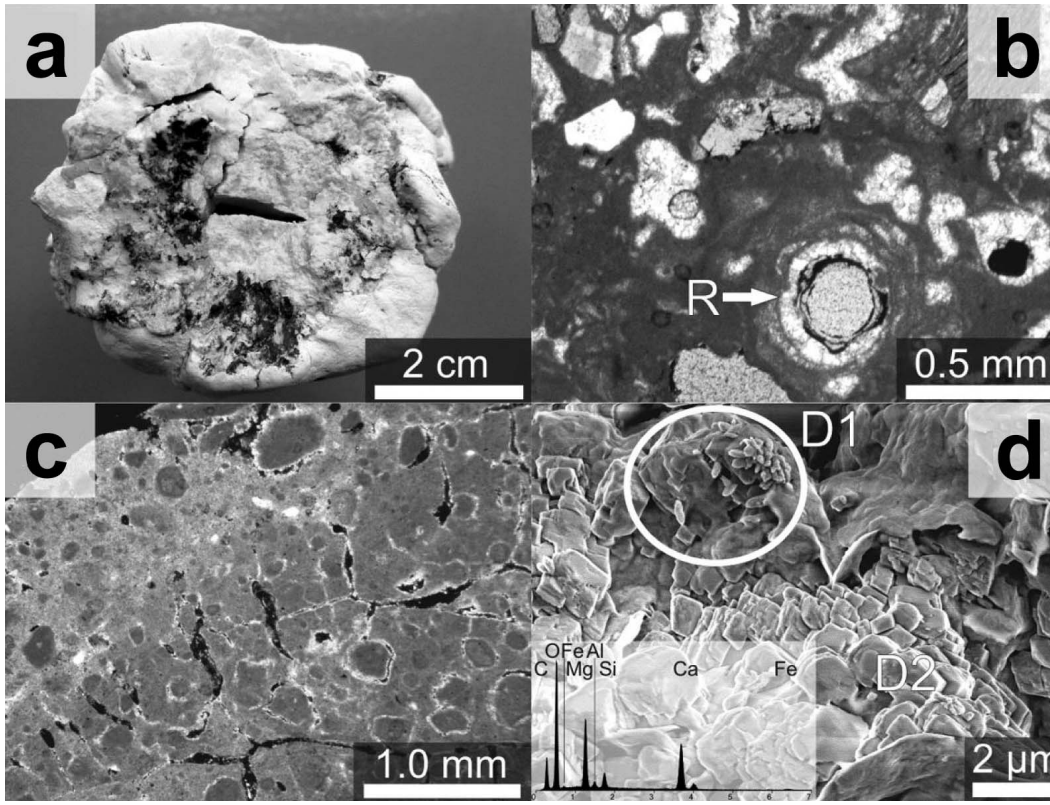

FIG. 3. Fabrics of pedogenic deposits. (a) Typical cracking and mottling of dolomite nodules. (b) Central root (R) channel in micritic dolomite; clay-lined and calcite-spar filled porosity. (c) Circumgranular cracks and brecciation fabrics with microspar at the edges. (d) Dolomitized sub-micron sized bacteria-like objects (D1) and micritic dolomite (D2).

Groundwater dolomite in deposits with pedogenic and palustrine carbonate

Groundwater dolomite can be present in the lower parts (Figs 2 and 4) of bentonite deposits (GB, UZ) either in the form of hard, elongated concretions up to 30 cm long with a pronounced core and white, powdery rim, and/or as fine-grained, clayey lenses with rare, aureoled quartz. Both concretions and clayey lenses are composed of cracked clotted micrite (M1) at the centre and dense microspar (M2) along cracks and rim. Cracks and different micrite generations point to a poly-phase formation history (Fig. 6a) and a connection of micritization and cracking. This could either be related to later micritization of clotted micrite (M1) and/or a second growth episode of concretions and clayey lenses (e.g. Wright & Tucker, 1991). Dolomite appears as rhombohedral crystals that replace residual grains in Fig. 6b. The variable grain size of dolomite rhombs of <1–6 μm, results in a clotted micrite appearance.

Pedogenic and groundwater calcite in bentonite deposits

Sub-ordinate calcite is present in some bentonite deposits (LD, H, ST) in varying abundance. While pedogenic calcite is morphologically identical to pedogenic dolomite, groundwater calcite shows some fabrics that are not found in pedogenic and palustrine environments and lack biogenic and desiccation features. In residual, only partially altered glass-bearing tuffite, calcite is found as small (1 cm) lentils or as granular calcite in root casts filled with smectite-rich, sandy sediment. In some bentonite deposits (H, ST), calcite is present as granular "sugary" nodules. The microfabrics of

https://doi.org/10.1180/claymin.2015.050.2.02 Published online by Cambridge University Press

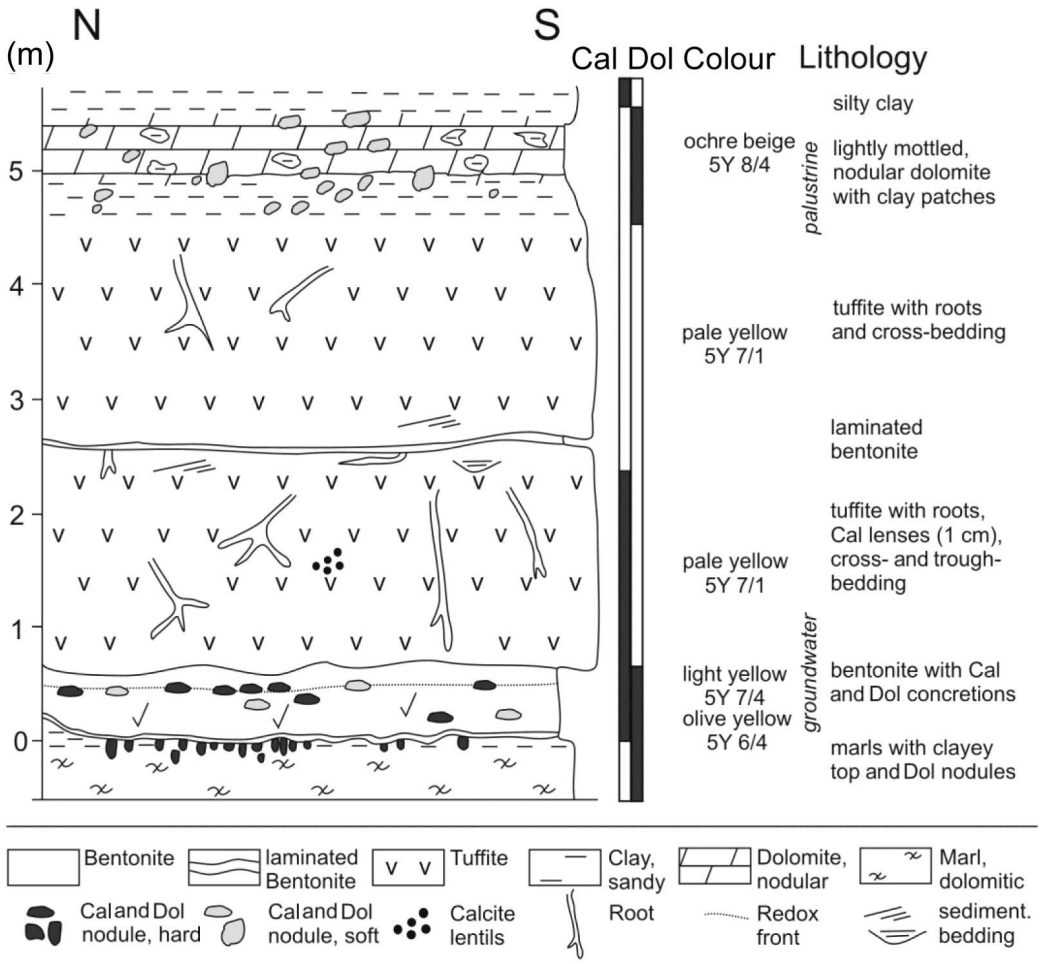

FIG. 4. Section of a bentonite deposit dominated by palustrine carbonates (Gabelsberg deposit). Cal = calcite, Dol = dolomite.

the groundwater calcites show a coarse, turbid calcite-spar, that is either the result of slow crystallization or the recrystallization of a precursor carbonate. Typical de-dolomitization fabrics such as rhomb-shaped open pores or pseudomorphs indicative of the recrystallization of a precursor dolomite are, however, lacking.

Mineralogical composition

X-ray diffraction analysis of the carbonates (Table 1, Fig. 7) reveals the presence mainly of dolomite and some calcite. The carbonate content was very variable, from 1–99 wt.%. Carbonates (Fig. 7) contain the same detrital, neoformed and residual volcanic minerals as bentonite and partially altered tuffite, i.e. smectite, illite/mica, quartz, feldspars, together with traces of kaolinite and chlorite and glass shards. A few of the dolomite nodules in the MB deposit and the partially altered tuffite in the GB deposit contained an undetermined silica phase (Fig. 5d). No minerals typical of terrestrial saline conditions, i.e. salts, gypsum, palygorskite or sepiolite were found, nor their dissolution fabrics (e.g. Talbot, 1990; Wright & Tucker, 1991).

STABLE ISOTOPES

Eighty two carbonate samples were analysed for their carbon and oxygen stable isotope compositions (Table 1). The average stable isotope composition

https://doi.org/10.1180/claymin.2015.050.2.02 Published online by Cambridge University Press

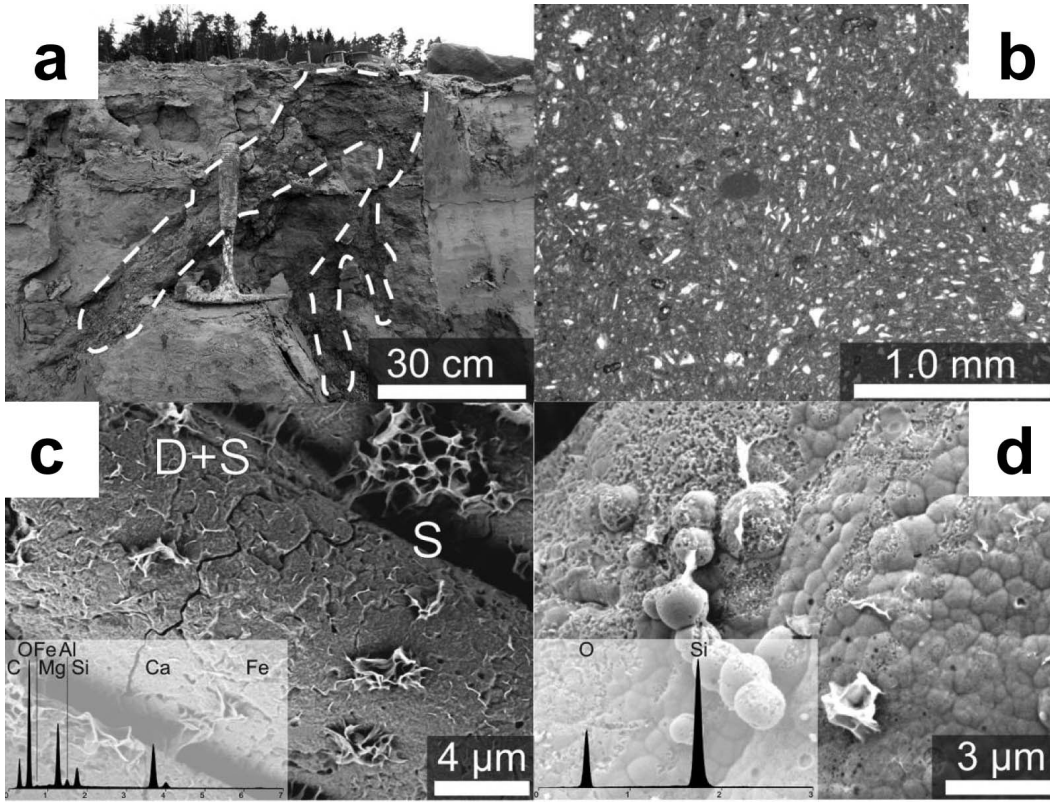

FIG. 5. Macro- and micro-fabrics in palustrine deposits. (a) Sediment-filled root in partially altered tuffite. (b) Soil churning fabrics, calcite in broken bioclasts and voids of dissolved volcanic glass particles. (c) Replacement of volcanic grains by granular dolomite and smectite (D+S), partially overgrown by smectite flakes (S). (d) Silica globules and smectite in partially altered tuffite. Note the solution pits and smectite crystallization within and on the silica globules.

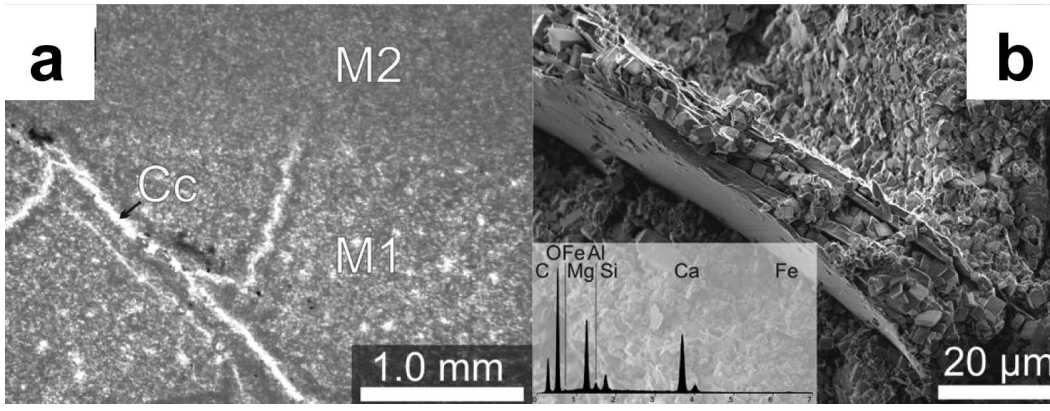

FIG. 6. Micro-fabrics of groundwater carbonates. (a) Dense (M2) and clotted (M1) micrite generations. Cracks filled with calcite (Cc). (b) Well preserved dolomite rhombs replacing a large mica flake.

https://doi.org/10.1180/claymin.2015.050.2.02 Published online by Cambridge University Press

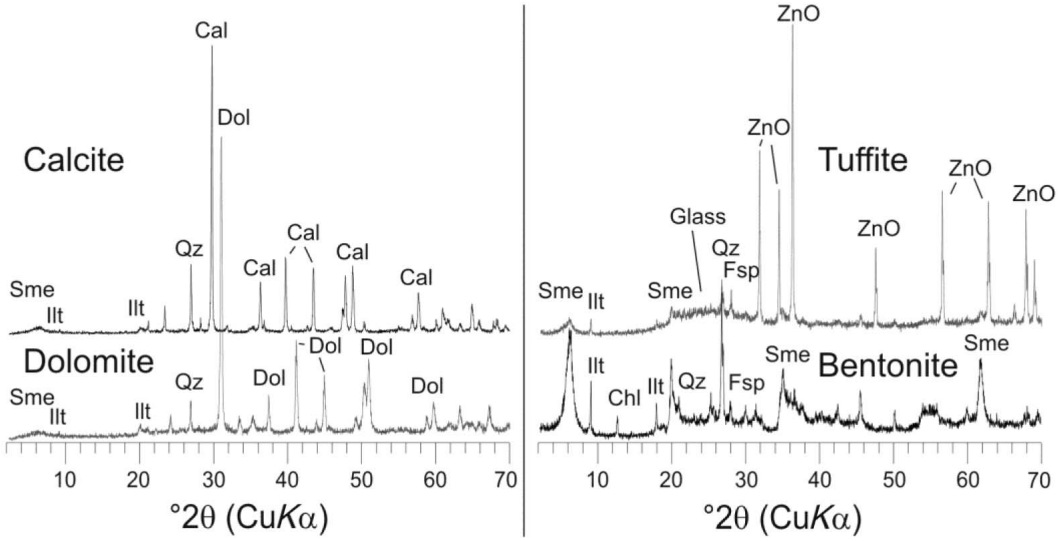

FIG. 7. Whole-rock XRD pattern of a calcite (ZW12) and a dolomite (GB10) nodule (left), as well as a tuffite and a bentonite (right). Cal = calcite, Dol = Dolomite, Sme = Smectite, Ilt = Illite/Muscovite, Qz = Quartz, Fsp = Feldspar, Chl = Chlorite and ZnO = zinc oxide (internal standard).

of the carbonates is shown in Table 2. Stable isotope ratios of calcite- or dolomite-rich end-members (>80 wt.%; n = 80) were used for a reconstruction of the environment of formation. The few calcite- and dolomite-bearing samples show an intermediate isotope composition (Table 1). The carbon and oxygen isotope ratios reveal distinct groups for pedogenic, palustrine and groundwater carbonate as illustrated in Fig. 8. The small amounts of dolomite and calcite found in the partially altered tuffite are isotopically identical to the carbonate from the bentonite. The carbonaceous wood recovered from the hanging-wall gravels of the Peterswahl deposit had a $\delta^{13}C$ value of -25.2 ± 0.2‰.

DISCUSSION

Pedogenic dolomite is very rare in the geological record and has been described in the basalt-derived Holocene soils of Hawaii, USA (Capo *et al*., 2000), the Permian fluviatile-lacustrine clastic sediments in the Ural mountains, Russia (Kearsey *et al*., 2012), and the Pleistocene petrocalcic soils in Spain (Diaz-Hernandez *et al*., 2013). Calcite and the small amounts of dolomite in the Cabo de Gata bentonites, Spain, have been described as pedogenic in origin (Delgado, 1993), while the calcite from Milos bentonite, Greece, is not derived from pedogenic processes (Decher *et al*., 1996). Dolomite in bentonite has not been examined systematically, but may yield new insights into the conditions and timing of bentonitization.

Carbonate formation and diagenetic setting

Terrestrial carbonates form in fresh to saline waters (Alonso-Zarza, 2003) in association with pedogenesis, activity of microorganisms and the root systems of plants (Wright & Tucker, 1991; Cerling & Quade, 1993) and their fabrics link them to processes closely related to the water table (Alonso-Zarza & Wright, 2010; Armenteros, 2010). Carbonates preserve indicators of palaeosol development, i.e. horizonation, root casts, mottling or gleying (Nettleton *et al*., 2000) present in practically all of the Bavarian bentonite deposits examined (Figs 2 and 4). Pedogenic (soil) and palustrine (lake wetlands) settings are home to deep rooting (Fig. 5a) vegetation (Alonso-Zarza, 2003). The preserved root fabrics (Fig. 3b), however, indicate that the soils were not permanently water-logged because most roots need oxygen to respire. The absence of permanently water-logged conditions and subsequent oxidation enhances ferruginization and mottling that are very common in upper bentonite horizons (Fig. 2) indicating the redistribution of iron during wet and dry cycles (Retallack,

https://doi.org/10.1180/claymin.2015.050.2.02 Published online by Cambridge University Press

TABLE 1. Mineral and stable isotope composition of dolomites and calcites. PED = pedogenic, PAL = palustrine, GW = groundwater, XXX = abundant, X = minor amounts, T = traces. Cal = calcite, Dol = dolomite, Sme = smectite, Ilt = illite/muscovite, Qz = quartz, Kln = kaolinite, Fsp = feldspar and Chl = chlorite.

Sample	Host Lithology	Type	$\delta^{18}O$	$\delta^{13}C$	Cal	Dol	Qz	Sme	Ilt	Kln	Chl	Fsp	Opal-CT	Amorph.
ZWEIKIRCHEN														
ZW031	Bentonitic clay	PED	−6.5	−8.1	48	5	41	3	3	–				
ZW029		PED	−4.5	−6.6	4	71	11	11	2	–				
ZW027		PED	−6.2	−8.5	33	7	35	15	9	1	T	T		
ZW002		PED	−5.1	−6.8	2	65	15	14	3	1				
ZW026		PED	−5.3	−6.5	0	95	3	1	1	1				
ZW025		PED	−5.4	−6.6	0	99	1	0	0	–				
ZW024		PED	−6.7	−9.0	78	8	6	6	2	–				
ZW023		PED	−5.0	−6.8	0	77	11	8	3	–		T		
ZW034	Bentonite	PED	−6.3	−6.2	4	45	21	24	6	–				
ZW006		PED	−4.9	−6.4	0	47	20	22	8	2				
ZW003		PED	−5.8	−6.6	0	50	28	13	7	1				
ZW005		PED	−5.1	−6.9	0	67	15	9	5	2				
ZW004		PED	−8.3	−10.7	75	1	10	9	4	1				
ZW022		PED	−5.1	−6.6	0	66	16	13	4	–				
ZW021		PED	−6.6	−8.8	60	5	13	15	7	1				
ZW020		PED	−5.1	−6.8	0	86	8	4	3	–				
ZW032		PED	−6.7	−8.9	64	6	8	16	7	–				
ZW018		GW	−6.4	−9.2	60	6	8	20	6	–				
ZW017		GW	−7.2	−9.4	70	0	5	19	6	–				
ZW016		PED	−7.1	−8.8	69	0	5	18	6	2				
ZW015		PED	−6.2	−9.2	75	2	9	8	5	–				
ZW033		PED	−7.4	−9.0	70	0	8	16	6	–				
ZW014		PED	−6.8	−9.2	24	2	6	62	6	–				
ZW013		PED	−3.4	−6.6	0	47	4	31	15	3		T		
ZW012		GW	−8.3	−11.5	80	0	2	15	2	1				
ZW011		GW	−9.1	−11.9	65	0	11	18	6	1	T			
ZW010		GW	−8.1	−11.3	73	0	3	19	3	2				
REHBACH														
RB03	Bentonite	PAL	−4.2	−7.5	3	36	5	50	7	–		T		
RB01		PAL	−4.6	−7.5	3	28	10	49	10	1		T		
RB04		PAL	−4.1	−7.1	0	68	3	24	4	–		T		
RB02		PAL			2	66	4	22	5	2		T		

LANDERSDORF											
LD06	Bentonite	GW	−7.6	−11.8	58	3	4	36	–	–	
LD05		PED	−7.9	−9.5	49	2	4	38	5	2	
LD04		PED	−7.3	−9.6	18	2	8	64	4	4	
LD03		PED	−7.4	−9.7	70	0	4	23	4	0	
LD02		GW	−7.1	−10.9	87	0	2	9	2	0	
LD01		PED	−7.0	−8.3	73	0	7	16	3	1	
GABELSBERG											
GB16	Dolomite bed	PAL	−3.5	−7.1	0	56	2	37	4	–	
GB34		PAL			4	58	6	27	5	–	
GB32		PAL	−3.9	−7.2	5	53	7	30	6	–	
GB10		PAL	−3.8	−7.1	2	70	4	19	5	–	
GB31		PAL	−6.1	−7.2	4	56	6	28	6	–	
GB09		PAL	−3.8	−7.2	0	56	5	24	15	–	
GB33		PAL	−4.1	−6.9	7	55	5	27	6	–	
GB30		PAL	−5.6	−6.9	7	44	8	33	8	–	
GB08		PAL	−3.5	−7.2	2	63	4	25	6	–	
GB22	Tuffite				3	0	18	68	11	–	
GB21					0	0	10	89	0	–	T
GB14		GW	−8.1	−10.6	8	0	5	83	3	–	
GB07					0	0	14	79	6	–	
GB06I		GW	−6.7	−11.7	XXX						
GB06II		GW	−6.7	−11.6	XXX						
GB06III		GW	−7.0	−11.7	XXX						
GB06		GW	−6.7	−11.4	45	0	7	37	10	–	
GB15	Bentonite	GW			3	3	6	79	9	–	
GB18		GW	−4.4	−7.1	2	43	3	49	4	–	
GB13		GW	−6.4	−10.8	58	11	4	24	3	–	
GB17		GW	−6.5	−10.8	84	6	1	8	1	–	
GB28		GW	−6.8	−11.0	86	2	1	10	2	–	
GB27		GW	−5.4	−7.4	32	35	4	27	2	–	
GB05		GW	−5.1	−6.4	0	33	4	57	5	–	
GB04		GW	−7.1	−10.9	34	19	4	40	4	–	
GB03		GW	−4.7	−7.1	0	68	2	26	4	–	
UNTERZELL											
UZ03	Bentonite	GW	−7.2	−10.4	85	2	3	8	2	T	
UZ04		GW			3	67	8	15	7	0	
UZ05		GW	−6.8	−9.0	86	0.4	3	7	2	2	
UZ01		GW	−4.8	−6.3	3	70	11	10	6	0	

Table 1 (*contd.*)

Sample	Host Lithology	Type	$\delta^{18}O$	$\delta^{13}C$	Cal	Dol	Qz	Sme	Ilt	Kln	Chl	Fsp	Opal-CT	Amorph.
HADER														
H05	Bentonite	GW			98	0	1		1					
H08		GW	−7.9	−11.1	97	0	1		1					0
H03		PED	−4.9	−7.7	0	48	3	33	7					8
H02		PED	−4.8	−7.3	0	37	3	38	12					9
H01		PED	−4.7	−7.5		58	2	28	4	T				8
H09		PED	−5.2	−6.5	0	37	8	22	20	T				13
H11		GW			XX	0								
H17		GW			XX	0								
H16		GW	−7.7	−11.7	97	0	T	T	T					
H13		GW			XX	0								
H12		PED	−5.5	−6.9	0	54	7	17	12					10
H10		PED	−5.1	−6.1	0	20	8	35	16					21
H15		PED	−5.0	−7.2	0	50	5	19	13					13
H14		PED	−5.0	−7.3	0	73	4	11	5					7
MITTERSBERG														
M29	Tuffite	PAL	−3.6	−7.3	0	65	T	17	3					14
M28	and	PAL	−3.4	−7.4	0	74	T	13	4	T				8
M27	Bentonite	PAL	−4.1	−7.4	0	75	T	13	3					8
M26		PAL			X	XX		XX						
M25		PAL	−4.8	−7.4	0	38	4	39	8	T	3	8		
M19		PAL	−5.0	−6.9	T	29	3	41	13		1			13
M18		PAL	−4.9	−7.4	0	66	3	21	6	1	2	1		
M13		PAL			0	1	3	64	14	1	3	9		4
M17		PAL	−4.2	−7.5	0	55	2	27	4	T				11
M14		PAL	−3.6	−7.3	0	60	2	25	4					9
M12	Tuffite	PAL	−3.8	−7.6	0	67	2	17	4	T				9
M10		PAL	−5.8	−8.0	5	10	3	57	16	1				8
M09		PAL	−4.3	−7.4	0	53	2	10	3					32
M11	Bentonite	PAL	−4.1	−7.0	0	35	18	17	9	1	3	3	6	8
M24	Footwall Marl		−4.0	−7.6	0	58	6	13	5				8	10
M23			−3.9	−7.1	0	61	3	5	3				9	19
M08			−4.0	−7.0	0	56	10	14	7		5	6	2	
M07			−4.2	−6.9	0	59	10	10	7		6	6	2	

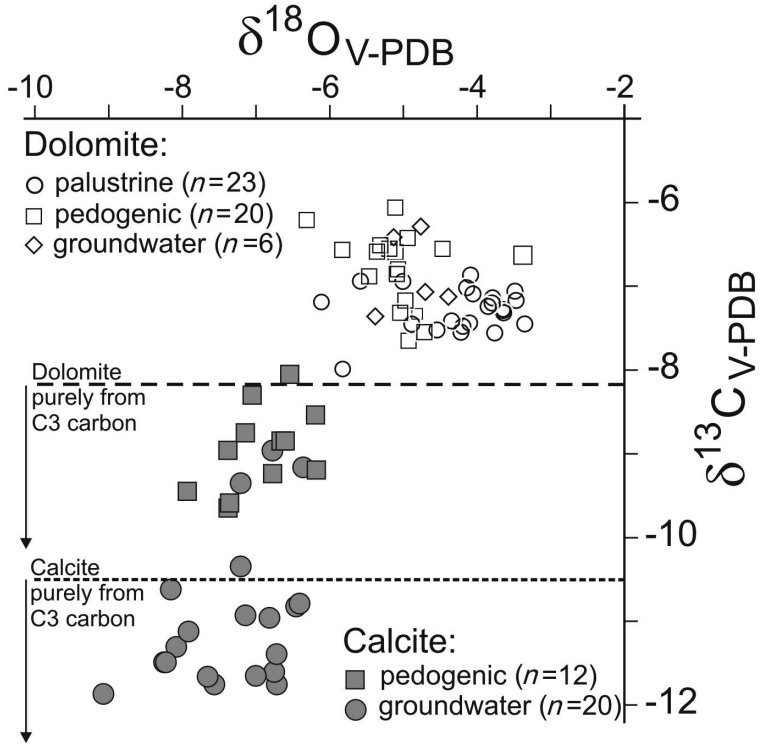

FIG. 8. Bivariate plot of oxygen and carbon stable isotope compositions of dolomite and calcite samples documented in Table 1. Dolomite and calcite limits, cf. *Carbon stable isotopes* below.

1988). Nodulization and pedoturbation (Figs 3b and 5b) fabrics due to the formation of curved and planar joint surfaces also point to repeated wetting and drying cycles (Freytet & Verrecchia, 2002). In contrast, grey clay patches underneath weakly mottled nodular dolomite (Fig. 4) indicate gleying and poor drainage (e.g. Freytet & Verrecchia, 2002).

Below the water table, groundwater carbonates form concretions with a diffuse boundary in the more protected phreatic zone (Wright & Tucker, 1991; Alonso-Zarza, 2003). In bentonites, earthy calcite-rich lenses (Fig. 2) and concretions (Fig. 4) may be present in footwall regions of bentonites, similar to valley calcrete (e.g. Wright & Tucker, 1991). Lenses and concretions are sometimes oriented horizontally along redox fronts between light and dark yellow oxidized bentonite (Fig. 4), probably reflecting the position of the water table.

Carbonate microfabrics are classified according to alpha- and beta-fabric end-members (Wright & Tucker, 1991). Alpha-fabrics lack biogenic forms and show a micritic to microsparitic groundmass, displacive growth, floating grains, or crystal-sized mottling. Beta-fabrics are dominated by biogenic features and signs of exposure or desiccation. Typical beta-fabrics are alveolar septal fabrics, circumgranular cracks, roots, coated grains, brecciation and clay cutans (Wright & Tucker, 1991). Intermediate forms of alpha- and beta-fabrics are common (Freytet & Verrecchia, 2002).

The palustrine and pedogenic carbonates in Bavarian bentonites reveal typical beta-fabrics. Palustrine carbonates show pedoturbation and broken bioclasts (Fig. 5b) typical for soil churning in wetlands (Freytet & Verrecchia, 2002), but they also show pedogenic fabrics, i.e. coalescent nodules, circumgranular cracks and shrinkage cracks (Fig. 3c), indicating soil rotation and desiccation in the vadose zone (Freytet & Verrecchia, 2002; Wright & Tucker, 1991). Alveolar septal fabrics of mineralized root walls (Klappa, 1980) were found in reworked bentonite (Fig. 2) and partially altered tuffite with partially

https://doi.org/10.1180/claymin.2015.050.2.02 Published online by Cambridge University Press

spar-filled root voids (Fig. 3b) indicating vadose conditions. The intimate growth fabric of granular dolomite and flaky smectite in partially altered tuffite (Fig. 5c) points to simultaneous or timely post-formational precipitation of carbonate and clay minerals. Elongated "rice" grains and aggregates that resemble fossil microbial remains are present in pedogenic dolomite (Fig. 3d). The size and shape of these grains are similar to either dolomite precipitated by moderately halophilic aerobic bacteria in culture experiments (Sánchez-Román *et al*., 2011) or to subrounded dolomite aggregates of spherical and oblong-shaped bodies in suboxic to oxic Pliocene lacustrine dolomite of the La Roda "white earths" from Spain (García del Cura *et al*., 2001). They are quite distinct from the dumbbell-shaped microbial dolomites precipitated in anoxic sulfate-reducing environments (Warthmann *et al*., 2000; van Lith *et al*., 2003) or the irregular masses and rods formed by methanogens (Roberts *et al*., 2004; Kenward *et al*., 2009). Although there is substantial debate on the nature of these objects, most authors agree on a microbial origin (e.g. Kirkland *et al*., 1999; Southam & Donald, 1999; Schieber & Arnott, 2003; Pacton *et al*., 2010; Sánchez-Román *et al*., 2011).

The groundwater carbonates show typical abiogenic alpha-fabrics. The micritic groundmass records a multi-phase formation and micritization history (Fig. 6a). The lack of porosity indicates a phreatic origin, while euhedral dolomites in clotted micrite and microspar (Fig. 6b) show steady formation processes (e.g. Wright & Tucker, 1991).

The macro- and microfabrics provide strong evidence for a syn- to very timely post-depositional formation of carbonates. Smectitization must have commenced shortly before or during carbonatization in order to explain the microfabrics discovered and their intimate intergrowth. The excellent primary fabric preservation rules out a later diagenetic overprint.

Carbon stable isotopes

The precipitation of soil carbonate is influenced by degassing, dewatering, evaporation, temperature and biological activity (e.g. Cerling, 1984; Wright & Tucker, 1991), but may show a seasonal bias caused by dry or warm periods (Cerling & Quade, 1993; Breecker *et al*., 2009; Passey *et al*., 2010). A fluctuating water table will therefore regulate both the decomposition of organic matter and mixing with atmospheric carbon dioxide. During non-waterlogged conditions atmospheric exchange is increased, leading to greater $\delta^{13}C$ values close to the palaeo-surface and increased evaporation. While the addition of Ca^{2+}, e.g. from inflowing water, enhances calcite formation, an increase of dissolved carbonate and/or evaporation will favour dolomite precipitation by either raising the CO_3^{2-}/Ca^{2+} and Mg/Ca ratios or the Mg and Ca concentrations (Machel & Mountjoy, 1986). In contrast, waterlogged water bodies are less affected by atmospheric exchange and often mirror either the carbon isotope composition of soil organic matter or the external input of dissolved carbonate (Talbot, 1990).

During the Mid-Miocene, C3-plants were the only significant organic carbon source in the UFM with an average $\delta^{13}C$ value of −25.5‰ (Tütken & Vennemann, 2009), similar to our result of −25.2±0.17‰. Based on the mean annual air temperature (MAT), estimated as 15−21ºC for the Mid-Miocene (Böhme, 2003; Böhme *et al*., 2007), calcites should be roughly 15‰ heavier than organic carbon (Cerling & Quade, 1993), suggesting an uppermost limit of calcite $\delta^{13}C$ values formed purely from C3-plant carbon of −10.6‰ (15ºC) to −11.3‰ (21ºC) (Fig. 8). Dolomite formed from C3-plant carbon (Fig. 8) only, should therefore have a $\delta^{13}C$ value of −8.2‰ (15ºC) to −8.9‰ (21ºC).

Dissolved inorganic carbon (DIC) introduced by groundwater is another important source of carbonate. For disseminated calcite with $\delta^{13}C$ values of +1.1 to +3.5‰ from Milos, Greece, Decher *et al.* (1996) suggested that dissolved inorganic carbon was sourced from overlying marine limestone. Delgado (1993) showed that dolomite in Cabo de Gata bentonite has $\delta^{13}C$ values of −5.8 to +1.8‰, indicating both marine and non-marine sources. In the Molasse basin Mesozoic marine lime and dolostone clasts have $\delta^{13}C$ values between −6.0 to +1.5‰, while UFM groundwaters show DIC $\delta^{13}C$ values of −15 to −9‰ (Egger *et al*., 1983). The carbon isotope values of carbonates in bentonites (Fig. 9a,b), however, do not match values expected from such soil CO_2 or DIC values alone (e.g. Romanek *et al.*, 1992). The $\delta^{13}C$ values of dolomite and calcite are, therefore, inconsistent with a single carbon source.

Considering a soil diffusional enrichment of 4.4‰, a pre-industrial atmospheric $\delta^{13}C$ value of −6.5‰ for the Mid-Miocene (Cerling, 1984; Cerling, 1991), calcite-CO_2 and calcite-HCO_3^-

https://doi.org/10.1180/claymin.2015.050.2.02 Published online by Cambridge University Press

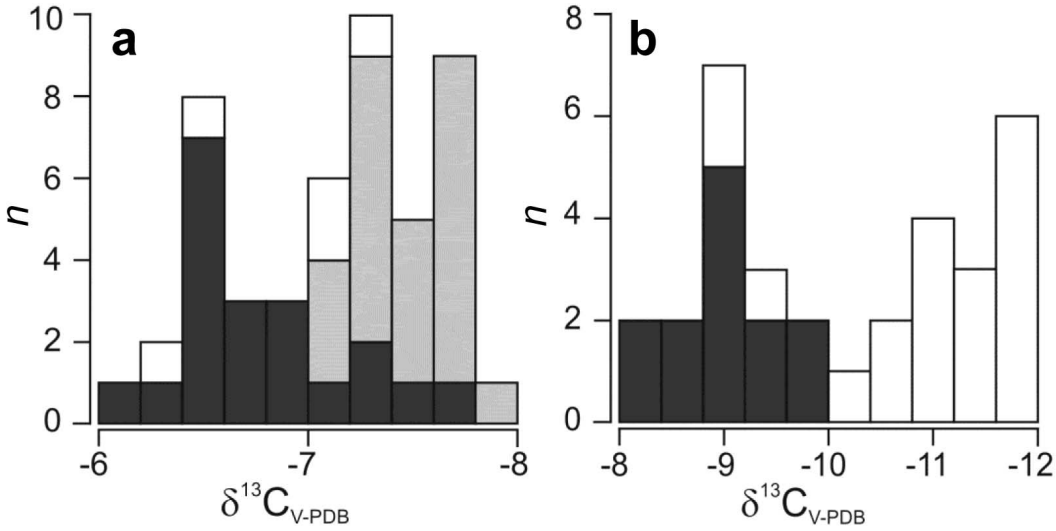

FIG. 9. (a) Carbon stable isotope histogram of dolomites; pedogenic (black), palustrine (grey), and groundwater carbonates (white). (b) Carbon stable isotope histogram of calcites; pedogenic (black) and groundwater carbonates (white). Data from Table 1.

fractionations of about 10.4‰ and 1‰ (Romanek *et al*.,1992), a simple mixing model of soil CO_2 with DIC or atmospheric CO_2 could account for the measured $\delta^{13}C$ values. This suggests that $\delta^{13}C$ values are probably the result of a soil CO_2-dominated three component system. In light of field relationships, mottling, shrinkage cracks and carbonate fabrics, a contribution of atmospheric carbon especially in pedogenic facies seems legitimate (e.g. Alonso-Zarza, 2003; García del Cura *et al*., 2001).

The carbon stable isotope results (Fig. 9a,b) are good indicators for fluctuating water levels with repeated changes between reducing wet (waterlogging during high stands) and oxygenated dry conditions. These conditions induced carbonate precipitation in warm/dry periods and supported smectite formation in wet periods. Incipient bentonites were settled by C3 vegetation that was the major source of carbon while minor amounts of carbon were derived from the atmosphere and carbonate-rich UFM groundwater.

Oxygen stable isotopes

Co-precipitated dolomite and calcite that has formed in oxygen isotope equilibrium should display a 3.1−4.4‰ fractionation at temperatures between 15−30ºC, which encompasses the estimates for MAT (15.7−20.8ºC) and the warm month temperatures (WMTs) of 20.2−28.1ºC (Böhme *et al*., 2007) and is consistent with the hydrogen and oxygen isotope data for the bentonite smectites (Gilg, 2005; Gilg & Rocholl, 2009; Bauer, 2014). We observed, however, an average oxygen isotope fraction between dolomite and calcite of 1.8‰ for pedogenic carbonates and 2.4‰ for groundwater carbonates (Table 2).

The $\delta^{18}O$ frequency distribution of carbonates (Fig. 10a,b) also illustrates a large scatter, indicating variable water compositions, temperatures or water sources. Co-precipitation in equilibrium would also have resulted in a more mixed carbonate composition; mixed dolomite-calcite samples are rare, however. We conclude that the dolomite and calcite must have formed either at different temperatures or in waters of differing isotopic compositions.

Tütken *et al*. (2006), Tütken & Vennemann (2009) and Héran *et al*. (2010) suggested that $\delta^{18}O_{V\text{-}SMOW}$ values in the upper soil column and in Mid-Miocene surface waters, of −5.9±1.7‰ or −5.6±0.7‰, were influenced by surface heating or evaporation based on mammal and turtle teeth phosphate. Gilg (2000) derived a $\delta^{18}O_{V\text{-}SMOW}$ value of approximately −7‰ for meteoric groundwater from Mid-Miocene kaolinite in southern Germany. These results show distinct isotopic differences between the palaeo-surface and more protected groundwater settings. The latter settings were found in bentonites meeting the conditions

https://doi.org/10.1180/claymin.2015.050.2.02 Published online by Cambridge University Press

TABLE 2. Stable isotope composition of dolomites and calcites.

	$\delta^{13}C_{V\text{-}PDB}$			$\delta^{18}O_{V\text{-}PDB}$		
	mean	min.	max.	mean	min.	max.
Pedogenic dolomite	−6.8 ± 0.4	−7.7	−6.1	−5.1 ± 0.5	−6.3	−3.4
Palustrine dolomite	−7.3 ± 0.3	−8.0	−6.1	−4.3 ± 0.7	−6.1	−3.4
Groundwater dolomite	−6.9 ± 0.4	−7.4	−6.3	−4.9 ± 0.3	−5.4	−4.4
Pedogenic calcite	−9.0 ± 0.5	−9.7	−8.1	−6.9 ± 0.5	−7.9	−6.2
Groundwater calcite	−10.9 ± 0.9	−11.9	−9.0	−7.3 ± 0.7	−9.1	−6.4

described by Hillel (1982), i.e. reduced surface heating and evaporation at depths >200 cm, which best reflect the MATs.

If groundwater calcite (n = 20) did precipitate at MAT and the conditions described above, it would have formed in water (Fig. 11) with a mean $\delta^{18}O_{V\text{-}SMOW}$ value of −7.0±0.7‰ (15ºC) to −5.7±0.7‰ (21ºC). As indicated by the similar range of $\delta^{18}O$ values (Fig. 10b), pedogenic calcite (n = 12) formed at similar conditions (Fig. 11) with a mean $\delta^{18}O_{V\text{-}SMOW}$ of water from −6.7±0.5‰ (15ºC) to −5.4±0.5‰ (21ºC), perhaps recording annual calcite formation being less affected by evaporation.

Untypical for extremely evaporative conditions, the ^{18}O values of dolomites are rather low (Fig. 8, Fig. 10a); lower than palustrine and pedogenic, microbially mediated dolomites formed at aerobic, moderately evaporative conditions in the La Roda white-earths that have dolomite $\delta^{18}O_{V-PDB}$ values of −3.07‰ to +5.40‰ (García del Cura *et al*., 2001). Traces of pedogenic dolomite present in Los Trancos bentonite also show high $\delta^{18}O_{V\text{-}PDB}$ values of between +0.5‰ and +3.3‰ (Delgado, 1993). Both occurrences indicate either more evaporative conditions and the involvement of non-marine water or a hydrothermal component (García del Cura *et al*., 2001; Delgado, 1993). In contrast calcite $\delta^{18}O_{V\text{-}PDB}$ values of −14.7‰ to −10.6‰ from Milos, Greece, were interpreted to have formed in hydrothermal mixed, meteoric-marine waters (Decher *et al*., 1996).

However, the carbon isotope values in Bavarian deposits show the dominance of soil CO_2 derived

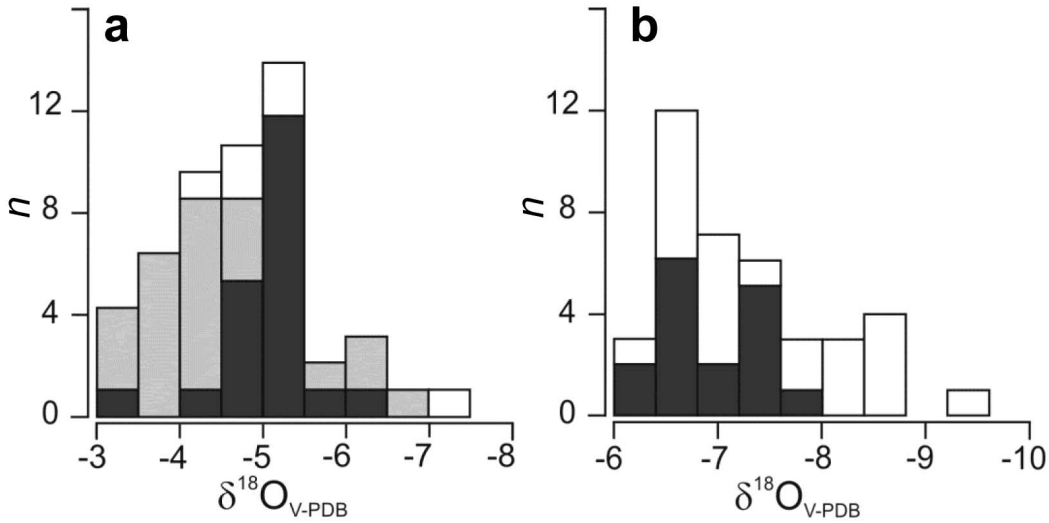

FIG. 10. (a) Oxygen stable isotope histogram of pedogenic (black), palustrine (grey), and groundwater (white) dolomites. (b) Oxygen stable isotope histogram of pedogenic (black), and groundwater (white) calcites. Data from Table 1.

https://doi.org/10.1180/claymin.2015.050.2.02 Published online by Cambridge University Press

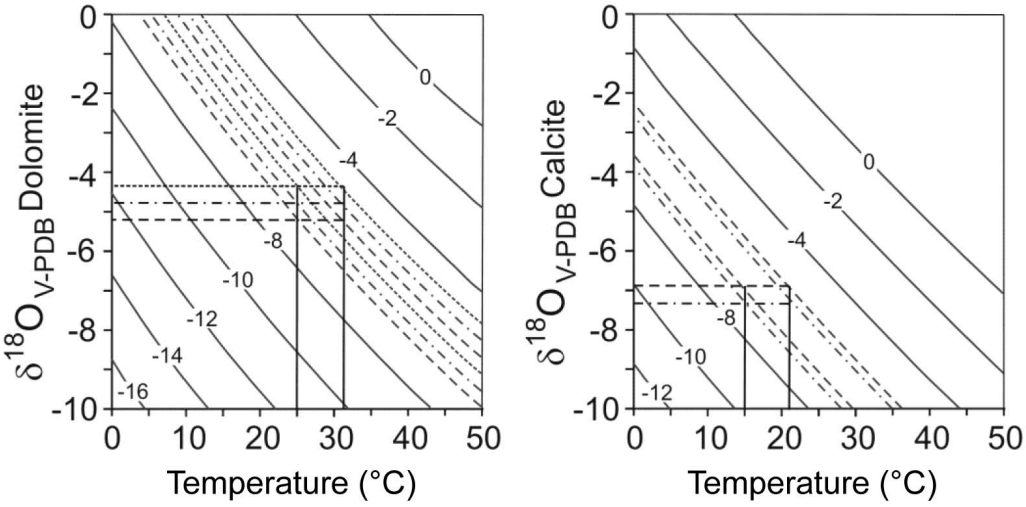

FIG. 11. Diagrams of oxygen isotope fractionation for dolomite-water (left) and calcite-water (right). Curves represent water $\delta^{18}O_{V\text{-}SMOW}$ values. Dotted, dotted-dashed and dashed lines represent oxygen isotope data of palustrine, ground and pedogenic waters. Black solid lines: upper and lower temperature limits (cf. *Oxygen stable isotopes*).

from the decomposition of organic matter, suggesting somewhat limited evaporation and degassing in comparison to conditions at La Roda and Los Trancos and the absence of marine waters. Cerling & Quade (1993) also argued that evaporation has little effect on $^{18}O/^{16}O$ ratios of soil water except for extreme environments, e.g. deserts or long surface exposure. Cerling & Quade (1993), Breecker *et al*. (2009) and Passey *et al*. (2010) used clumped isotopes to extend this notion and Quade *et al.* (2013) described a 10–15ºC summer bias of carbonate based MATs compared to WMTs, for shallow depths (200 cm). As a consequence the isotopic composition of water in upper soil layers is controlled by temperatures 10–15ºC above MAT resulting in conservatively estimated temperatures of 25–31ºC. These temperatures reflect ground temperatures slightly above the WMT (20.2–28.1ºC; Böhme *et al*., 2007). Applying these temperatures (Fig. 11) in equation 1 (Vasconcelos *et al*., 2005), pedogenic dolomite (n = 20) would have precipitated in waters with a similar average isotopic composition as calcites of −6.8±0.6‰ (25ºC) to −5.6±0.6‰ (31ºC), while palustrine dolomites (n = 23) experience stronger evaporation (e.g. Alonso-Zarza, 2003) and therefore formed in slightly enriched waters of −6.0±0.8‰ to −4.8±0.8‰. The few groundwater (n = 5) dolomites would have formed in waters of −6.4±0.3‰ to −5.2±0.3‰, questioning their true groundwater nature and suggesting mixing with downward percolating waters.

Oxygen isotope values of calcite and dolomite are similar to those found by Tütken *et al*. (2006), Tütken & Vennemann (2009) and Héran *et al*. (2010) and confirm that carbonates in bentonite formed in meteoric ground- and surface waters. The good agreement of calcite with MATs and meteoric water might suggests calcite precipitation throughout the year. In contrast, pedogenic and palustrine dolomite formation were probably intense in hot/dry periods when temperature and evaporation were greatest.

CARBONATE FORMATION AND ITS RELATIONSHIP TO BENTONITIZATION

Dolomitization and smectitization of Mg-poor rhyolitic ash required the introduction of Mg^{2+} and Ca^{2+} ions (e.g. Folk & Land, 1975; Christidis, 2008). Hydrothermal, strongly evaporated or saline fluids did not exist in the UFM (Vogt, 1980; Ulbig, 1999; Unger, 1999; Schmid, 2002; Abdul-Aziz *et al*., 2009). These new stable isotope results confirm that dolomite and calcite in bentonites formed from meteoric waters. The present-day meteoric groundwaters in the UFM are of Ca–Mg–HCO_3 type (Egger *et al*., 1983, Table 3) and similar to Ca–(Mg–)–HCO_3 waters involved in the formation of the Northern Cabo de Gata bentonites, such as Los Trancos (Caballero *et al*., 2005).

https://doi.org/10.1180/claymin.2015.050.2.02 Published online by Cambridge University Press

The groundwater in the UFM show variable Mg^{2+} (0.05 mmol/L to 1.98 mmol/L) and Ca^{2+} (0.05 to 3.35 mmol/L) concentrations and also variable molar Mg/Ca ratios (0.53 to 1.57; Table 3) that are consistent with the stability of calcite and in part dolomite (Folk & Land, 1975; Machel & Mountjoy, 1986). The average molar Mg/Ca ratio of the UFM ground waters (~0.86) is in equilibrium with the molar interlayer Mg/Ca ratio in smectites of the Bavarian bentonites (0.51; Grim & Güven, 1978) considering the preferential uptake of Ca relative to Mg in the interlayer of smectites (e.g., Laudelout *et al*., 1968; Sayles & Mangelsdorf, 1979).

Additionally, the weathering of limestone and dolostone in Molasse sediments (Egger *et al*., 1983) and the decomposition of soil organic matter (e.g. Talbot, 1990), enhanced carbonate formation by raising the pH and carbonate alkalinity (CO_3^{2-}/Ca^{2+} ratio). Machel & Mountjoy (1986) contended that the increased carbonate alkalinity is equally as important for dolomitization as a high Mg/Ca ratio because it shifts the reaction kinetics towards dolomite. Although sulfate reduction might have enhanced dolomite formation, sulfate is not *per se* a kinetic inhibitor to dolomite precipitation. The low sulfate concentrations do, however, provide conditions suitable for dolomite precipitation (e.g. Last, 1990; Sánchez-Román *et al*., 2011). During the Mid-Miocene, $Ca-Mg-HCO_3^-$ water in the Molasse basin was probably a large reservoir of Mg^{2+} and Ca^{2+} derived from dissolution of limestone and dolostone clasts, cation-exchange with clay minerals (Egger *et al*., 1983) and possibly silicate weathering. The presence of dolomite in bentonites, therefore, indicates that waters with high carbonate alkalinity and Mg/Ca ratios around 1 percolated through incipient soils and volcanic ash.

CONCLUSIONS

Carbonates in bentonites were examined systematically for the first time and their relationship to bentonitization was explored. The new petrographic and isotope geochemical data show that pedogenic and palustrine dolomite and calcite are important constituents of non-marine bentonite deposits in Bavaria.

Carbonates formed below and above a fluctuating groundwater table. Plants, groundwater and soils provided the biological background, the Mg/Ca ratio and the carbonate alkalinity, respectively, required for dolomite formation in a strictly non-arid environment. Silica globules in the carbonates show that silica mobility and dolomitization were a coeval process, while the intimate intergrowth of smectite and dolomite point to either a syngenetic or at least very timely post-smectitization process. While dolomitization and smectitization started at about the same time it cannot be ruled out that smectitization continued after blanketing of deposits by younger sediment.

Bentonitization of acidic, Mg- and Ca-poor volcanic precursor rocks does not necessarily require the involvement of seawater or saline conditions. It was a terrestrial process driven by $Ca-Mg$-rich waters influenced by pedogenesis. The strong pedogenic imprint implies that bentonitization occurred soon after deposition on a time scale similar to that of the development of soils.

ACKNOWLEDGMENTS

This publication is part of the first author's Ph.D. research at the Lehrstuhl für Ingenieurgeologie at the Technische Universität München, Germany. Prof. Dr Christopher Mayr at the section of Palaeontology & Geobiology of the Ludwig-Maximilians-Universtität and Dr Ulrich Struck, Museum of Natural History in Berlin enabled the stable isotope analyses. We are grateful for access to bentonite mines granted by Bernhard Ratzke, Süd-Chemie AG (now Clariant), and the cooperation of Hans-Ulrich Boehnke, S&B Industrial Minerals. Dr Jürgen Bär, Institut für

TABLE 3. Composition of groundwater in the Upper Freshwater Molasse (Egger *et al*., 1983).

Water type	$Ca-Mg-HCO_3$
Mg/Ca ratio (molar)	0.53 to 1.37
pH	7.26 to 9.10
Carbonate alkalinity (CO_3^{2-} or HCO_3^- /Ca^{2+})	>>2.5
Sulfate (mmol/L)	0 to 0.8
Total dissolved solids (mg/L)	280±51

https://doi.org/10.1180/claymin.2015.050.2.02 Published online by Cambridge University Press

Materialwissenschaften, Universität der Bundeswehr München, gave access to the field-emission scanning electron microscope. Also acknowledged is B.Sc. student Adrian Richter for field work and XRD analyses from samples of the Mittersberg and Hader deposits. We are grateful for the efforts of the two reviewers whose comments improved the manuscript considerably and the useful remarks of the editor. This study was supported financially by the Society of Economic Geologists', SEG Graduate Fellowship Award 2012.

REFERENCES

Abdul Aziz H., Böhme M., Rocholl A., Zwing A., Prieto J., Wijbrans J.R., Heissig K. & Bachtadse V. (2009) Integrated stratigraphy and $^{40}Ar/^{39}Ar$ chronology of the Early to Middle Miocene Upper Freshwater. *International Journal of Earth Sciences*, **97**, 115–134.

Alonso-Zarza A.M. (2003) Palaeoenvironmental significance of palustrine carbonates and calcretes in the geological record. *Earth-Science Reviews*, **60**, 261–298.

Alonso-Zarza A.M. & Wright, V.P. (2010) Calcretes. Pp. 225–267 in: *Carbonates in Continental Settings: Facies, Environments and Processes* (A.M. Alonso-Zarza & L.H. Tanner, editors). Developments in Sedimentology, **61**. Elsevier, Amsterdam.

Armenteros, I. (2010) Diagenesis of Carbonates in Continental Settings. Pp. 61–151 *Carbonates in Continental Settings: Geochemistry, Diagenesis and Applications* (A.M. Alonso-Zarza & L.H. Tanner, editors). Developments in Sedimentology, **62**, Elsevier, Amsterdam.

Bauer K. (2014) Stable O and H isotopic composition of hydrous minerals as proxies for paleoclimate and topography: Application to the European Alps. PhD thesis, Université de Lausanne, Switzerland. Pp. 304–305.

Böhme M. (2003) The Miocene Climatic Optimum: Evidence from ectothermic vertebrates of Central Europe. *Palaeogeography, Palaeoclimatology, Palaeoecology*, **195**, 389–401.

Böhme M., Bruch A.A. & Selmeier A. (2007) The reconstruction of Early and Middle Miocene climate and vegetation in Southern Germany as determined from the fossil wood fauna. *Palaeogeography, Palaeoclimatology, Palaeoecology*, **253**, 91–114.

Breecker D.O., Sharp Z.D. & McFadden L.D. (2009) Seasonal bias in the formation and stable isotopic composition of pedogenic carbonate in modern soils from central New Mexico, USA. *Geological Society of America Bulletin*, **121**, 630–640.

Caballero E., de Cisneros C.J., Huertas F.J., Huertas F., Pozzuoli A. & Linares J. (2005) Bentonites from Cabo de Gata, Almería, Spain: a mineralogical and geochemical overview. *Clay Minerals*, **40**, 463–480.

Capo R.C., Whipkey C.E., Blachère J.R. & Chadwick O.A. (2000) Pedogenic origin of dolomite in a basaltic weathering profile, Kohala peninsula, Hawaii. *Geology*, **28**, 271–274.

Cerling T.E. (1984) The stable isotopic composition of soil carbonate and its relationship to climate. *Earth and Planetary Science Letters*, **71**, 229–240.

Cerling T.E. (1991) Carbon dioxide in the atmosphere: Evidence from Cenozoic and Mesozoic paleosols. *American Journal of Science*, **291**, 377–400.

Cerling T.E. & Quade J. (1993) Stable carbon and oxygen isotopes in soil carbonates. *Geophysical Monograph Series*, **78**, 217–231.

Christidis G. (2008) Do bentonites have contradictory characteristics? An attempt to answer unanswered questions. *Clay Minerals*, **43**, 515–529.

Christidis G. & Dunham A.C. (1997) Compositional variations in smectites; Part II, Alteration of acidic precursors, a case study from Milos Island, Greece. *Clay Minerals*, **32**, 253–270.

Christidis G. & Huff W.D. (2009) Geological aspects and genesis of bentonites. *Elements*, **5**, 93–98.

Decher A., Bechtel A., Echle W., Friedrich G. & Hoernes S. (1996) Stable isotope geochemistry of bentonites from the island of Milos (Greece). *Chemical Geology*, **129**, 101–113.

Deines P. (2004) Carbon isotope effects in carbonate systems. *Geochimica et Cosmochimica Acta*, **68**, 2659–2679.

Delgado A. (1993) Estudio isotópico de los procesos diagenéticos e hidrotermales relacionados con la génesis de bentonitas (Cabo de Gata, Almería). PhD thesis, Universidad Granada, Spain, Pp. 91–113.

Delgado A. & Reyes E. (1993) Isotopic study of the diagenetic and hydrothermal origins of the bentonite deposits at Los Escullos (Almería, Spain). Pp. 675–678 in: *Current research in Geology Applied to Ore Deposits*, (P. Fenoll Hach-Ali, J. Torres-Ruiz & F. Gervilla, editors), University of Granada, Spain.

Diaz-Hernandez J.L., Sánchez-Navas A. & Reyes E. (2013) Isotopic evidence for dolomite formation in soils. *Chemical Geology*, **347**, 20–33.

Egger R., Eichinger L., Rauert W. & Stichler W. (1983) Untersuchung zum Grundwasserhaushalt des Tiefenwassers der Oberen Süßwassermolasse durch Grundwasseraltersbestimmung. *Informationsberichte Bayerisches Landesamt für Wasserwirtschaft*, **8/83**, 99–145.

Folk R.L. & Land L.S. (1975) Mg/Ca ratio and salinity: two controls over crystallization of dolomite. *American Association of Petroleum Geologists Bulletin*, **59**, 60–68.

Freudenberger W. & Schwerd K. (1996) Erläuterungen zur Geologischen Karte von Bayern 1:500000.

Bayerisches Geologisches Landesamt. Pp. 1–329.
Freytet P. & Verrecchia E.P. (2002) Lacustrine and palustrine carbonate petrography: an overview. *Journal of Paleolimnology*, **27**, 221–237.
García del Cura M.A., Calvo J.P, Ordonez S., Jones B.F. & Canaveras J.C. (2001) Petrographic and geochemical evidence for the formation of primary, bacterially induced lacustrine dolomite: La Roda 'white earth' (Pliocene, central Spain). *Sedimentology*, **48**, 897–915.
Gilg H.A. (2000) D-H evidence for the timing of kaolinization in Northeast Bavaria, Germany. *Chemical Geology*, **170**, 5–18.
Gilg H.A. (2005) Eine geochemische Studie an Bentoniten und vulkanischen Gläsern des nordalpinen Molassebeckens (Deutschland, Schweiz). Pp. 16–18 in: *Berichte der deutschen Ton- und Tonmineralgruppe e.V., Beiträge zur Jahrestagung Celle 10.–12. Oktober 2005*, (R. Dohrmann, editor), Deutsche Ton- und Tonmineralgruppe, Köln, Germany.
Gilg H.A. & Rocholl A. (2009) The bentonite puzzle: a stable isotope and geochemical perspective, p. 87 in: *Abstracts of the 46th Annual Meeting of the Clay Minerals Society*, Clay Minerals Society, Billings.
Grim R.E. & Güven, N. (1978) Origin of bentonites. Pp. 126–137 in: *Bentonites: Geology, Mineralogy, Properties and Uses* (R.E. Grim & N. Güven, editors). Developments in Sedimentology, **24**, Elsevier, Amsterdam.
Héran M.A., Lécuyer C. & Legendre S. (2010) Cenozoic long-term terrestrial climatic evolution in Germany tracked by $\delta^{18}O$ of rodent tooth phosphate. *Palaeogeography, Palaeoclimatology, Palaeoecology*, **285**, 331–342.
Hillel D. (1982) *Introduction to Soil Physics*. Academic Press, New York. Pp. 155–167.
Hofmann B. (1973) Geologische Karte von Bayern 1:25000, Erläuterungen zum Blatt Nr. 7439 Landshut Ost. Pp. 44–50.
Kearsey T., Twitchett R.J. & Newell A.J. (2012) The origin and significance of pedogenic dolomite from the Upper Permian of the South Urals of Russia. *Geological Magazine*, **149**, 291–307.
Kenward P.A., Goldstein R.H., Gonzáles L.A. & Roberts J.A. (2009) Precipitation of low temperature dolomite from an anaerobic microbial consortium: the role of methanogenic Archaea. *Geobiology*, **7**, 556–565.
Kim S.T. & O'Neil J.R. (1997) Equilibrium and nonequilibrium oxygen isotope effects in synthetic carbonates. *Geochimica et Cosmochimica Acta*, **61**, 3461–3475.
Kirkland B.L., Lynch F.L., Rahnis M.A., Folk R.L., Molineux I.J. & McLean R.J.C. (1999) Alternative origins for nannobacteria-like objects in calcite. *Geology*, **27**, 347–350.
Klappa C.F. (1980) Rhizoliths in terrestrial carbonates: classification, recognition, genesis and significance. *Sedimentology*, **27**, 613–629.
Last W.M. (1990) Lacustrine dolomite – an overview of modern, Holocene, and Pleistocene occurrences. *Earth-Science Reviews*, **27**, 221–263.
Laudelout H., van Bladel R., Bolt G.H. & Page A.L. (1968) Thermodynamics of heterovalent cation exchange reaction in a montmorillonite clay. *Transactions of the Faraday Society*, **64**, 1477–1488.
Lemcke K. (1973) Zur nachpermischen Geschichte des nördlichen Alpenvorlandes. *Geologica Bavarica*, **69**, 5–48.
Machel H.-G. & Mountjoy E.W. (1986) Chemistry and environments of dolomitization – a reappraisal. *Earth-Science Reviews*, **23**, 175–222.
Nettleton W.D., Olson C.G. & Wysocki D.A. (2000) Paleosol classification: Problems and solutions. *Catena*, **41**, 61–92.
Pacton M., Gorin G., Vasconcelos C., Gautschi H.P. & Barbarand J. (2010) Structural arrangement of sedimentary organic matter: nanometer-scale spheroids as evidence of a microbial signature in early diagenetic processes. *Journal of Sedimentary Research*, **80**, 919–932.
Passey B.H., Levin N.E., Cerling T.E., Brown F.H. & Eiler J.M. (2010) High-temperature environments of human evolution in East Africa based on bond-ordering in palaeosol carbonates. *Proceedings of the National Academy of Science*, **107**, 11245–11249.
Quade J., Eiler J., Daëron M. & Achyuthan H. (2013) The clumped isotope geothermometer in soil and paleosol carbonate. *Geochimica et Cosmochimica Acta*, **105**, 92–107.
Retallack G.J. (1988) Field recognition of palaeosols. Pp. 1–20 in: *Paleosols and Weathering through Geologic Time: Principles and Applications*. Geological Society of America Special Paper, **216**, (J. Reinhardt & W.R. Sigleo, editors). Boulder, Colorado, USA.
Roberts J.A., Bennett P.C., González L.A., Macpherson G.L. & Milliken K.L. (2004) Microbial precipitation of dolomite in methanogenic groundwater. *Geology*, **32**, 277–280.
Romanek C.S., Grossmann E.L. & Morse J.W. (1992) Carbon isotopic fractionation in synthetic aragonite and calcite: Effects of temperature and precipitation rate. *Geochimica et Cosmochimica Acta*, **56**, 419–430.
Rosenbaum J. & Sheppard S.M.F. (1986) An isotopic study of siderites, dolomites and ankerites at high temperatures. *Geochimica et Cosmochimica Acta*, **50**, 1147–1150.
Sánchez-Román M., Romanek C.S., Fernández-Remolar D.C., Sánchez-Navas A., McKenzie J.A., Pibernat R.A. & Vasconcelos C. (2011) Aerobic biomine-

alization of Mg-rich carbonates: Implications for natural environments. *Chemical Geology*, **281**, 143–150.

Sayles F.L. & Mangelsdorf P.C. Jr. (1979) Cation-exchange characteristics of Amazon River suspended sediment and its reaction with seawater. *Geochimica et Cosmochimica Acta*, **43**, 767–779.

Schieber J. & Arnott H.J. (2003) Nanobacteria as a by-product of enzyme-driven tissue decay. *Geology*, **31**, 717–720.

Schmid W. (2002) *Ablagerungsmilieu, Verwitterung und Paläoböden feinklastischer Sedimente der Oberen Süßwassermolasse Bayerns*. Bayerische Akademie der Wissenschaften Abhandlungen, Heft 172, PhD thesis, Ludwig-Maximilians-Universität, Germany. Pp. 170–185.

Sheppard S.M.F. & Schwarcz H.P. (1970) Fractionation of carbon and oxygen isotopes and magnesium between coexisting metamorphic calcite and dolomite. *Contributions to Mineralogy and Petrology*, **26**, 161–198.

Southam G. & Donald R. (1999) A structural comparison of bacterial microfossils vs. 'nanobacteria' and nanofossils. *Earth-Science Reviews*, **48**, 251–264.

Talbot M.R. (1990) A review of the palaeohydrological interpretation of carbon and oxygen isotopic ratios in primary lacustrine carbonates. *Chemical Geology, Isotope Geoscience Section*, **80**, 261–279.

Tütken T., Vennemann T.W., Janz H. & Heinzmann E.P.J. (2006) Palaeoenvironment and palaeoclimate of the Middle Miocene lake in the Steinheim basin, SW Germany: A reconstruction from C, O, and Sr isotopes of fossil remains. *Palaeogeography, Palaeoclimatology, Palaeoecology*, **241**, 457–491.

Tütken T. & Vennemann T.W. (2009) Stable isotope ecology of Miocene large mammals from Sandelzhausen, southern Germany. *Paläontologische Zeitschrift*, **83**, 207–226.

Ulbig A. (1999) Untersuchungen zur Entstehung der Bentonite in der bayerischen Oberen Süßwassermolasse. *Neues Jahrbuch Geologisch-Paläontologische Abhandlungen*, **214**, 497–508.

Unger H.J. (1999) Die tektonischen Strukturen der bayerischen Ostmolasse. *Documenta Naturae*, **125**, 1–16.

van Lith Y., Warthmann R., Vasconcelos C. & McKenzie J.A. (2003) Sulphate-reducing bacteria induce low-temperature Ca-dolomite and high Mg-calcite formation. *Geobiology*, **1**, 71–79.

Vasconcelos C., McKenzie J.A., Warthmann R. & Bernasconi S.M. (2005) Calibration of the $\delta^{18}O$ paleothermometer for dolomite precipitated in microbial cultures and natural environments. *Geology*, **33**, 317–320.

Vogt K. (1980) Bentonite Deposits in Lower Bavaria. *Geologisches Jahrbuch*, **D39**, 47–68.

Warthmann R., van Lith Y., Vasconcelos C., McKenzie J.A. & Karpoff A.M. (2000) Bacterially induced dolomite precipitation in anoxic culture experiments. *Geology*, **28**, 1091–1094.

Wright V.P. & Tucker M.E. (1991) Calcretes: an introduction. Pp. 1–25 in: *Calcretes*. (V.P. Wright & M.E. Tucker, editors). The International Association of Sedimentologists, Reprint Series no. 2. Blackwell Scientific Publications, Oxford, UK.

https://doi.org/10.1180/claymin.2015.050.2.02 Published online by Cambridge University Press